Effect of Specimen Size on Small Punch Creep Behavior of High Nitrogen Ferritic Heat-Resistant Steels

Naveena, Shin-ichi Komazaki

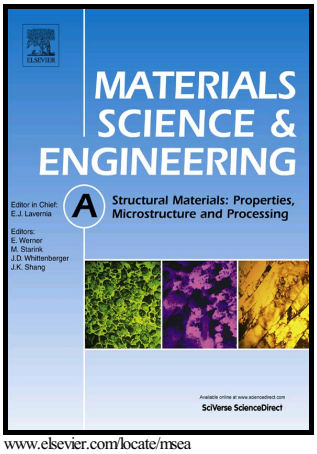

www.elsevier.com/locate/msea

PII: S0921-5093(18)30216-8
DOI: https://doi.org/10.1016/j.msea.2018.02.030
Reference: MSA36117

To appear in: *Materials Science & Engineering A*

Received date: 1 August 2017
Revised date: 6 February 2018
Accepted date: 7 February 2018

Cite this article as: Naveena and Shin-ichi Komazaki, Effect of Specimen Size on Small Punch Creep Behavior of High Nitrogen Ferritic Heat-Resistant Steels, *Materials Science & Engineering A,* https://doi.org/10.1016/j.msea.2018.02.030

Effect of Specimen Size on Small Punch Creep Behavior of High Nitrogen Ferritic Heat-Resistant Steels

Naveena[*] and Shin-ichi Komazaki[**]

[*]*Division of Mechanical Engineering*
Graduate School of Science and Engineering, Kagoshima University, Japan, 890-0065
[**]*Research Field in Engineering, Science and Engineering Area*
Research and Education Assembly, Kagoshima University, Japan, 890-0065

ABSTRACT

The small punch (SP) creep tests were carried out on different high nitrogen ferritic heat-resistant steels in the temperature range of 650-800 ˚C, in the load range of 55-400 N, using disc-type specimens measuring ∅8×0.5 mm (∅8 mm) and ∅3×0.25 mm (∅3 mm). The influence of specimen size on SP creep behavior and on the conversion of SP creep rupture results to conventional uniaxial creep rupture results were investigated. The creep deflection and rupture life of ∅3 mm specimens were much smaller/shorter than those of the ∅8 mm specimens. The experimentally determined SP load-uniaxial stress conversion coefficients to correlate SP and uniaxial creep rupture life were different for the two specimens; 2.05 and 0.49 for ∅8 mm and ∅3 mm specimens, respectively. These observed effects were considered as virtual specimen size effects as these could occur not only due to specimen size but also due to geometrical parameters of the test rig. The conversion coefficients were found to be independent of the type of steels investigated. The conversion coefficients determined from finite element analysis, 2.03 and 0.47 for ∅8 mm and ∅3 mm specimens, respectively, were in close agreement with those obtained from experimental results. Based on the close agreement between the experimental creep rupture life and that predicted using finite element

[*]Corresponding author. Tel.: +81-99-285-8159; fax: +81-99-285-8245.
E-mail address: naveena@mech.kagoshima-u.ac.jp

analysis results, it was found that there was no significant actual specimen size effect on the creep rupture life.

Keywords: Small punch creep; Specimen size effect; High nitrogen ferritic steels; Load-stress conversion coefficient

1. Introduction

The small punch (SP) creep testing technique is an effective method of characterizing creep behavior of materials especially (a) when material for testing is available in limited quantity during the design and development of new alloys [1, 2], (b) in the case where removal of sample material large enough to fabricate conventional uniaxial creep test specimen from operating component is not desirable for residual life assessment studies [3, 4] and (c) when evaluation of creep properties of narrow heat-affected zones of welded joints is desired [5]. The technique has attracted the attention of several research groups worldwide who have been working on its standardization [4, 6–12]. At present, the specimen and rig dimensions employed by different research groups are different due to the fact that the technique is not standardized [12]. The diameter (or size of square/rectangular specimen) and thickness of specimen vary from 3 to 10 mm and 0.25 to 0.5 mm, respectively [12]. Accordingly, the indenter diameter (1 to 2.5 mm) and rig dimensions also vary [12]. These geometrical parameters are expected to influence SP creep test results. A few studies on the influence of specimen thickness/diameter, indenter diameter, rig parameters, test atmosphere, loading speed, etc. on SP creep behavior of materials have been reported [13–15]. Nakata et al. [16] carried out finite element analysis and investigated the effect of specimen size on small punch creep property of RAFM steel. Their study showed that the SP specimen dimensions, both thickness and diameter, affect the SP creep rupture time and fracture deflection. However, the availability of experimental results in the literature on specimen size effect, either on SP creep test result or its conversion to uniaxial creep test result, is quite scarce. There are some studies on the specimen size effect in the case of miniature creep specimens. Kanayama et al. [17] studied the specimen size effect on creep properties of a Mod. 9Cr-1Mo steel using tensile bulk specimens in different test environments like argon gas, air and vacuum. Their study revealed that there was no effect of specimen size on the creep rupture life. However, they observed that the testing environment influenced the creep rupture life. Itoh et al. [18] investigated creep rupture behavior of Mod. 9Cr-1Mo, 2.25Cr-1Mo steels, 304 and 316

stainless steels using miniature creep specimens and compared the results with those obtained from the standard creep specimens. The study revealed that there was no specimen size effect on the creep rupture life. Zhang et al.[19] found that the creep deformation and rupture behavior of Gr.91 steels determined from miniature creep specimens were comparable to those determined from the standard creep specimens which indicated no specimen size effect.

In order to standardize the SP creep test technique, it is essential to establish a thorough understanding of the effect of influence parameters on both SP creep test result and its conversion to uniaxial creep test result. In view of this, an effort has been made in the present study to investigate the effect of specimen size on the SP creep test result and its conversion to uniaxial creep test result. The SP creep testing using TEM disc-type specimen having dimension ∅3×0.25 mm was developed by Komazaki et al. [3] for characterizing creep rupture properties of the heat-affected zones of welded joints. This type of specimen was originally employed for characterizing tensile properties [20–22]. In the present study, both ∅3×0.25 mm and ∅8×0.5 mm specimens were used to examine the effect of specimen size on creep deformation and rupture behavior of the steels and its dependence on the correlation between SP and conventional uniaxial creep test results. This effect was investigated in different heats of high nitrogen ferritic heat-resistant steels which vary by its chemical compositions, heat treatment conditions and microstructures in order to examine their influence on the specimen size effect. The size effect was analyzed based on the results obtained from experiments and finite element analyses.

2. Experimental procedure

2.1 Materials and creep tests

The chemical compositions and heat treatment conditions of the high nitrogen ferritic heat-resistant steels used in the present study are given in Table1. The details of microstructure of these steels have been reported previously [1]. The steels 1 and 2, which were normalized and tempered, essentially had a tempered martensitic microstructure. The steel 3 which was only normalized consisted of a fully ferrite microstructure. Steels 1 and 2 had same chemical compositions but were subjected to different heat treatment conditions with an original intent of studying their influence on creep rupture strength [1]. As mentioned previously, these steels were considered in this study to clarify whether there is any dependence of size effect on their microstructures and/or heat treatment conditions. The SP creep tests were conducted

at different temperatures in the range of 650-800 ˚C, under different loads in the range of 55-400 N using two different sized SP specimens measuring ∅8×0.5 mm (∅8 mm) and ∅3×0.25 mm (∅3 mm). Both surfaces of the specimens were ground and polished upto a final mirror finish using 0.3 μm Al_2O_3. The thickness of both specimens was carefully controlled to achieve the specified thickness with a tolerance less than 1 %. The SP creep test rigs employed for ∅8 mm and ∅3 mm specimens are schematically shown in Figs. 1a and b, respectively. The test specimen was clamped between the upper and lower dies and a constant load was applied to the specimen through a Si_3N_4 spherical ball indenter. During the test, the central deflection was measured using linear variable differential transducer (LVDT). The SP creep tests were performed in a flowing argon (99.99 % pure) atmosphere within the specimen chamber in order to prevent severe oxidation of the specimen-rig assembly. The test temperature was maintained constant with an accuracy of ±1 ˚C.

2.2 Finite element analysis

The Finite element (FE) analyses of SP creep test were carried out to examine the stress-state in the SP specimen and to investigate the relationship between SP load and uniaxial stress. Two-dimensional axisymmetric models for simulation of SP creep tests of ∅8×0.5 mm and ∅3×0.25 mm specimens were developed using FEA software ABAQUS standard 6.11 [3]. An example of ∅8×0.5 mm FE model is shown in Fig. 2. The specimens were modeled as deformable bodies and meshed using linear quadrilateral elements of type CAX4R. The specimen mesh size was 0.04×0.05 mm in the case of ∅8×0.5 mm specimen and 0.025×0.025 mm in the case of ∅3×0.25 mm specimen. These mesh sizes were used to get more accurate results. It was confirmed that using mesh size smaller than this produced no significant difference in the results. The indenter and dies, which were much stiffer than the specimen, were modeled as perfectly rigid bodies. To the ball indenter, a displacement/rotation boundary condition was applied so as to allow its displacement only in the loading direction. The lower die was fixed by constraining all displacements and rotations at the reference point indicated in Fig. 2. The displacements of nodes of the specimen on the axisymmetric axis were constrained to move along the axisymmetric axis. The specimen is clamped between the upper and lower die by applying a force to the upper die at the reference point indicated in Fig.2. The SP creep tests were simulated by considering elastic-plastic-creep analysis. In the present FE model, the elastic, plastic and creep properties of a conventional high Cr ferrtic

steel (Gr.91[23]) were used in the simulation because of an insufficient material properties available for these new high nitrogen steels. This approximation with respect to the material properties was made based on the result of our previous study which showed that the conventional and these new high nitrogen steels have same SP load-uniaxial stress conversion coefficient of 2.05 [1]. The reason for the same load-stress conversion coefficients applicable for the conventional steel Gr.91 and the high nitrogen steels is the creep ductilities of these steels which fall in a range where the load-stress conversion coefficient remains same. This was confirmed from the previous study of the variation of load-stress conversion coefficients with equivalent fracture strain (indicative of creep ductility) by Komazaki et al. [24]. The study showed that for certain high temperature alloys, including Gr.91 steel, having relatively higher creep ductility values, the load-stress conversion coefficient values remain same. The properties of the steel (Gr.91[23]) used in the FE model are given in Table 2. The creep deformation was simulated by using Norton's power law constitutive equation. The coulomb friction between the indenter and specimen was considered to be 0.39 and those between the specimen and dies (upper and lower) were assumed to be 0.5. The simulations were carried out under constant loads in the range 220-400 N applied on the reference point (RP) of the indenter, at 650 ˚C.

3. Results and discussion

3.1 Influence of specimen size on creep deformation and rupture behavior

Figure 3 shows the typical central deflection-time behavior (SP creep curve) and central deflection rate-time behavior measured on ∅8 mm specimen of steel 2, at 103 N/750 ˚C. The creep curves exhibited clear primary, secondary and tertiary creep regions. The deflection rate rapidly decreased upon loading in the primary creep region. In the secondary creep region, the deflection rate remained almost constant. This region was followed by a tertiary creep region characterized by an accelerating deflection rate culminating with rupture of the specimen. Figures 4a and b show the SP creep curves measured on ∅8 mm and ∅3 mm specimens, respectively, at 700 ˚C under different loads in steel 2. Both specimens exhibited qualitatively similar creep curves as described in Fig. 3. However, they exhibited a relatively large difference in the central deflection which indicates difference in the creep rupture ductility of the two specimens. The ∅8 mm specimen showed much higher total deflection of ≈2.5 mm than the ∅3 mm specimen where the central deflection was ≈0.7 mm. This result

was consistent with the finite element analysis results reported by Nakata et al. [16]. They found that the creep fracture deflection increased with increasing specimen thickness. The cause of the above difference could be both the specimen dimensions and different diameters of the indenters which imparted different stresses to the specimen for an applied load. However, the influence of diameter of the receiving hole which may have some possible effects on the central deflection could not be studied here. The central deflection at rupture was almost independent of the applied load, test temperature and time to rupture in both specimens. The secondary creep stage was relatively longer in both specimens.

Figures 5a-d show the comparison of fracture morphology of ∅8 mm and ∅3 mm specimens observed in steel 3 after creep testing at 700 ^{o}C. Both specimens were found to be ruptured circumferentially (Figs. 5a and b). A typical ductile transgranular mode of fracture was observed in both specimens (Figs. 5c and d). The fracture morphology in other two steels were also found to be similar. Figure 6 shows the comparison of SP creep rupture results obtained from ∅8 mm and ∅3 mm specimens of the three steels, analyzed using Larson-Miller parametric (LMP) method [25]. The rupture life of ∅8 mm specimens was longer than that of the ∅3 mm specimens even when the applied loads were approximately same. This effect is in agreement with the finite element analysis results reported by Nakata et al. [16], who found that the creep rupture time increased with increasing specimen thickness. Therefore, this effect could be attributed to the different thickness of the specimen. However, it is also important to note that the ball indenter diameter used in two specimens were different due to which the stresses imparted to the specimens for an applied load were different. As a result, the difference in rupture time could also be caused by these different stresses. Therefore, these observed differences including the above discussed central deflections could be considered as virtual size effects because these could occur not only due to different specimen sizes but also due to different stresses aroused on account of different ball diameters for a given applied load and temperature. There was no significant difference in the creep rupture strength between the three steels.

3.2 Influence of specimen size on load-stress conversion coefficient

The correlation between the rupture life of SP and uniaxial creep test can be achieved by converting the load applied in SP creep test to the stress applied in uniaxial creep test which

provides an equivalent rupture life using a load-stress conversion coefficient. The relationship between the SP load (F) and uniaxial stress (σ) can be expressed as,

$$F = \alpha\sigma \quad (1)$$

where α is load-stress conversion coefficient. The load-stress conversion relationships for both ∅8 mm and ∅3 mm specimens were determined by performing regression analysis on the SP and uniaxial creep rupture results (stress versus LMP plot), by varying α between 2 and 3 in the case of ∅8 mm specimen, and between 0.4 and 0.6 in the case of ∅3 mm specimen. Based on the maximum value of regression coefficient of determination (r^2_{max}), which yielded the best fit, the conversion coefficients were determined to be 2.05 and 0.49 for the ∅8 mm and ∅3 mm specimens, respectively. Figures 7a-c show the results of correlation between the SP and uniaxial creep rupture life for ∅8 mm and ∅3 mm specimens, using experimentally determined load-stress conversion coefficients. The SP creep rupture results were in relatively good agreement with the uniaxial creep rupture results, although some scatter (less than 5%) can be seen in steel 3 (Fig. 7c). The similar scatter was also be observed in the uniaxial creep test results (less than 5%) (Fig. 7c) , the cause of which is not yet known. At high stress levels the variation seems to have a different slope than that in the lower stress levels. Because of inadequate uniaxial creep rupture results in the high stress regime the cause for the slope change at high stress regime could not be identified.

The FE analysis was performed to analyze the stress-state in the SP creep test specimen, more specifically to determine relationship between the stress-state in the secondary creep region and the applied load. A typical comparison of the SP creep curves obtained from the experiment and FE analysis for ∅8 mm specimen is shown in Fig.8. Both creep curves were in good agreement which indicated the validity of FE model. As mentioned above, since the simulation of creep deformation considered only the secondary creep properties, and creep crack initiation and propagation were not taken into account, the tertiary creep region of the FE creep curve was not in agreement with the experimental one (220 N). The stress analysis revealed that the Von-Mises stress reached maximum at a location away from the centre of specimen in the radial direction, where the fracture is likely to occur, as shown in Fig. 9. The maximum Von-Mises stress generally occurs in the specimen close to its contact boundary with ball indenter and the location shifts in the radial direction as the contact area between the specimen and indenter increases. Figure 10 shows the variation of average Von-Mises stress (average equivalent stress) with creep time for

different SP loads in ∅8 mm specimen. The average Von-Mises stress was calculated along the thickness direction of the specimen at a location where the maximum Von-Mises stress existed (Fig. 9) on the outer surface of the specimen. At first, this location was identified after the completion of creep simulation. Then, at this location at a creep time corresponding to secondary stage creep was chosen to calculate the average Von-Mises stress. Further, at this location, the average Von-Mises stress was considered because there was only a marginal difference between the maximum Von-Mises stress at the outer surface and the minimum Von-Mises stress at the inner surface of the specimen along the thickness direction. As can be seen, the Von-Mises stress, after an initial abrupt decrease, attained a constant value which remained constant during most of the creep time until the onset of acceleration creep stage. This constant stress is likely to control the creep deformation and fracture behavior of the specimen, and seems to be a stress equivalent to uniaxial creep stress which provides a rupture time equivalent to that of the SP creep test. Further, this region of the curve where the average equivalent stress was constant appeared to be corresponding to the steady-state creep region. It is interesting to note that the central deflection rate-time behavior shown in Fig. 3 resembled the average equivalent stress-time behavior shown in Fig. 10, exhibiting a steady creep deflection rate and a constant equivalent stress. The average equivalent stress increased with increase in load. There was a linear relationship between the equivalent stress (σ_s) and the SP load (F) in both specimens which can be seen in Fig. 11, in Gr.91 steel. These relationships were determined to be,

$$F_{\phi 8} = 2.03\sigma_s \tag{2}$$

$$F_{\phi 3} = 0.47\sigma_s \tag{3}$$

It was found that the load-stress conversion coefficients determined from the FE analysis were in reasonably good agreement with the experimentally determined load-stress conversion coefficients. From our previous study, it can be noted that the load-stress conversion coefficient for the conventional Gr.91 steel was same as that of the high nitrogen steels [1]. Therefore, consideration of the material properties of Gr.91 steel in the FE simulation did not significantly affect the result of load-stress conversion relationships for high nitrogen steels. From the experimental and FE analysis results, it can be seen that the load-stress conversion coefficients were different for ∅8 mm and ∅3 mm specimens. This indicates that the load-stress conversion coefficient depends on the specimen size. Further, the load-stress conversion coefficient also depends on the material properties of the specimen.

A recent study by Komazaki et al. [24] showed that the creep ductility of specimen material affects the load-stress conversion coefficient. They observed that the load-stress conversion coefficient increased with increase in creep ductility up to a certain value of creep ductility and beyond which it remained almost constant. Further, the analytical equations for the load-stress conversion coefficient suggest that in addition to the specimen dimension, the ball diameter and other geometrical parameters of the test rig also affect the load-stress conversion coefficient [2, 26]. This is discussed in the following section. Therefore, from the viewpoint of all the above mentioned influence parameters the effect of specimen size on the load-stress conversion coefficient can also be regarded as virtual specimen size effect. The load-stress conversion coefficients were found to be same for the three steels, although these steels had different microstructures, namely, martensite (steel 1 and 2) and fully ferrite (steel 3), different chemical compositions, mainly with respect to Cr and V contents, and different heat treatment conditions. This result revealed that the load-stress conversion coefficients were not influenced by the type of microstructures, variation in the chemical compositions and heat treatment conditions of these high nitrogen steels.

3.3 Size effect on creep rupture property

The dependence of load-stress conversion coefficient on other geometrical parameters such as radius of the ball and receiving hole of the lower die was analyzed. A schematic illustration of the deformation of specimen in SP creep test is shown in Fig. 12. The effective sectional area (in mm^2) of the specimen represents the load-stress ratio, F/σ, which is equal to the load-stress conversion coefficient α (in mm^2). The effective sectional area depends on the specimen thickness. Therefore, the load-stress conversion coefficient of ∅8×0.5 mm specimen is higher than that of the ∅3×0.25 mm specimen. An equation relating F and σ, proposed in Chakrabarty's membrane stretching model [26] can be expressed as,

$$F/\sigma = 2\pi h\left[R + \frac{h}{2}\right]\sin^2\phi \tag{4}$$

where F is the SP load, σ is the membrane stress, R is the radius of the ball, h is the thickness of specimen and ϕ is the angle between the load axis and the line connecting the center of ball and the point of maximum stress in the deformed specimen. This equation indicates that the load-stress conversion coefficient depends on the specimen thickness, the radius of ball and the angle ϕ. According to the European Code of Practice (CoP) [2], the load-stress conversion

ratio depends also on the radius of receiving hole in the lower die in addition to the other geometrical parameters. The proposed relationship was,

$$F/\sigma = 3.33 k_{sp}\, r^{-0.2} R^{1.2} h \tag{5}$$

where, k_{sp} is the ductility constant of the specimen material, r is the radius of receiving hole in the lower die, R is the radius of the ball and h is the specimen thickness.

In the present study, the creep rupture life was taken as a parameter to analyze the actual size effect. From Eqns. 4 and 5, the ratios of load-stress conversion coefficients for the specimen-indenter geometry used in the present study, assuming that the angle ϕ is same in both specimens, can be calculated as,

$$\left[\frac{F_{\phi 8}/\sigma}{F_{\phi 3}/\sigma}\right]_{Chak.} = 4.67 \tag{6}$$

$$\left[\frac{F_{\phi 8}/\sigma}{F_{\phi 3}/\sigma}\right]_{CoP} = 4.57 \tag{7}$$

Similarly, the ratios of load-stress conversion coefficients obtained from the experimental results and FE analysis can be calculated as,

$$\left[\frac{F_{\phi 8}/\sigma}{F_{\phi 3}/\sigma}\right]_{Exp.} = 4.18 \tag{8}$$

$$\left[\frac{F_{\phi 8}/\sigma}{F_{\phi 3}/\sigma}\right]_{FE} = 4.32 \tag{9}$$

A comparison of the load-stress conversion coefficient ratios determined using the analytical equations, FE model and experimental results is shown in Table 3. The ratios determined from the Chakrabarty's model (Eqn 6), CoP (Eqn 7) and FE analysis (Eqn 9) were used to estimate the load-stress conversion coefficient for ∅3 mm specimen by considering the load-stress conversion coefficient 2.05 of ∅8 mm specimen. Then, the estimated load-stress conversion coefficient of ∅3 mm specimen was used to predict creep rupture life of ∅3 mm specimen. Figure 13 shows the comparison of the experimental creep rupture life and predicted creep rupture life (using Eqn 6, 7 and 9) for ∅3 mm specimen, analyzed using LMP method. As can be seen in Fig. 13, the experimental creep rupture life was in close agreement with that predicted using the FE analysis (Eqn 9). This result of close agreement indicated that there existed no significant actual specimen size effect. This result could be regarded as an actual specimen size effect because of the fact that the actual specimens consisted of

several microstructural features mainly grains size, grain boundaries, block/lath boundaries etc but the similar features were not taken into account in the FE model. And despite this fact, the FE analysis result was in close agreement with the experimental one. The results obtained in the present study were consistent with the results reported in the literatures on the effect of specimen size in Mod. 9Cr-1Mo [17, 18], 2.25Cr-1Mo steels [18] and Gr.91 steel [19]. The observed relatively large difference between the experimental creep rupture life and that predicted using Eqns 6 and 7 (Chakrabarty's model and CoP) could be due to the assumptions/approximations made in these equations and it needs further investigations for a clear understanding. For future studies of the specimen size effect on creep rupture property, these results provide insight into the load-stress conversion coefficients for the two specimens and these coefficients can be used to conduct SP creep tests on both specimens at same equivalent stress and temperature which enables direct comparison of their creep rupture life.

From the metallurgical point of view, as the test specimen is miniaturized the influence of microstructural features on the characterized material property becomes an important factor. One of the prime metallurgical features is the number of grains that a specimen consists in order to represent a bulk or standard size specimen. The number of grains in the specimen can cause the size effect on the creep properties, more importantly in those alloys where grain size is relatively large, for instance in austenitic stainless steels and Ni-base alloys. In the case of ferritic steels, where the grain size is relatively smaller, even further miniaturized SP specimen (∅3 mm) is likely to contain sufficient number of grains for deformation process to be able to represent ∅8 mm SP specimen. The grain size of the steels studied was 30-40 μm. The approximate number of grains contained in the thickness direction were 12-16 and 6-8 in a ∅8 mm and ∅3 mm specimen, respectively. Based on the results obtained in this study, a further miniaturized SP specimen (∅3 mm) can be used to characterize creep properties of ferritic and ferritic-martensitic steels.

4. Conclusions

The small punch creep behavior of the high nitrogen ferritic heat-resistant steels was investigated using ∅8×0.5 mm and ∅3×0.25 mm specimens. The influence of specimen size on SP creep behavior and on the correlation between SP and uniaxial creep rupture results were analyzed. The creep deflection and time to rupture were found to be influenced by the specimen size. The load-stress conversion coefficients to correlate SP creep rupture life to

that of the uniaxial one were different for the two specimens; 2.05 and 0.49 for ∅8×0.5 mm and ∅3×0.25 mm specimens, respectively. These effects of specimen size were considered as virtual specimen size effects as these could occur not only due to specimen size but also due to other geometrical parameters of the test rig. The load-stress conversion coefficients were not dependent on whether the microstructure of the steel was tempered martensite or ferrite, and also it was independent of their heat treatment conditions. The conversion coefficients determined from the finite element analysis, 2.03 and 0.47 for ∅8 mm and ∅3 mm specimens, respectively, were in close agreement with those obtained from the experimental results. As a results of this and based on the close agreement between the creep rupture life obtained from the experiment and that predicted using finite element analysis results, it was found that there was no significant actual specimen size effect on the creep rupture life.

Acknowledgments

This work was carried out as part of the research activities of ALCA (Advanced Low Carbon Technology Research and Development Program). The financial support received from JST (Japan Science and Technology Agency) for this project is greatly acknowledged. The authors sincerely thank the project Head and members for providing the uniaxial creep data for comparison.

References

[1] Naveena, S. Komazaki, Evaluation of creep rupture strength of high nitrogen ferritic heat-resistant steels using small punch creep testing technique, Mater. Sci. Eng. A 676 (2016) 100-108.

[2] M.D. Mathew, J. Ganesh Kumar, V. Ganesan, K. Laha, Small punch creep studies for optimization of nitrogen content in 316LN SS for enhanced creep resistance, Metall. Mater. Tran. A. 45 (2014) 731-737.

[3] S. Komazaki, T. Sugimoto, T. Hasegawa, Y. Kohno, Damage evaluation of a welded joint in a long-term service-exposed boiler by using a small punch creep test, ISIJ International. 47 (8) (2007) 1228-1233.

[4] B. Ule, T. Sustar, F. Dobes, K. Milicka, V. Bicego, S. Tettamanti, K. Maile, C. Schwarzkopf, M.P. Whelan, R.H. Kozlowski, Small punch test method assessment for the

determination of the residual creep life of service exposed components: outcomes from an interlaboratory exercise, Nucl. Eng. Design. 192 (1999) 1-11.

[5] S. Komazaki, T. Kato, Y. Kohno, H. Tanigawa, Creep property measurements of welded joint of reduced-activation ferritic steel by the small punch creep test, Mater. Sci. Eng. A 510-511 (2009) 229-233.

[6] J.D. Parker, J.D. James, International Conference on Developments in Progressing Technology, American Society for Mechanical Engineers, 1994, 279, pp. 167–72.

[7] S. Komazaki, T. Hashida, T. Shoji, K. Suzuki, Development of small punch tests for creep property measurement of tungsten-alloyed 9%Cr ferritic steels, ASTM J. Test. Eval. 28 (2000) 249-256.

[8] R. Hurst, K. Matocha, Proceedings of Second Conference on Small Sample Test Techniques: Determination of Mechanical Properties of Materials by Small Punch and Other Miniature Testing Techniques, Ostrava, Czech Republic, 2012, pp. 4-18.

[9] D.T. Blagoeva, R.C. Hurst, Application of the CEN (European Committee for Standardization) small punch creep testing code of practice to a representative repair welded P91 pipe, Mater. Sci. Eng. A 510–511 (2009) 219-223.

[10] Small Punch Test Method for Metallic Materials Part 1: A Code of practice for small Punch testing at elevated temperatures, Report No. CEN/WS 21, 2005.

[11] F. Dobeš, K. Milička, On the Monkman-Grant relation for small punch test data, Mater. Sci. Eng. A 336 (2002) 245-248.

[12] Standard for Small Punch Creep Test-Estimation of Residual Life for High Temperature Component, JSMS, Report No. ISBN978-4-901381-38-3, 2012.

[13] T. Nakata, S. Komazaki, Y. Kohno, H. Tanigawa, Development of a small punch testing method to evaluate the creep property of high Cr ferritic steel: Part I-Effect of atmosphere on creep deformation behavior, Mate. Sci. Eng. A 666 (2016) 54-60.

[14] Z. Zhou, Y. Zheng, X. Ling, R. Hu, J. Zhou, A study on influence factors of small punch creep test by experimental investigation and finite element analysis, Mater. Sci. Eng. A. 527 (2010) 2784-2789.

[15] K. Kobayashi, M. Kaneko, H. Koyama, G.C. Stratford, M. Tabuchi, Deformation and fracture in small punch creep tests, and influence factors on creep rupture life (Testing Environment and Radius of Lower Die), Trans. Japan Society of Mechanical Engineers A, 77(784) (2011) 2046-2053.

[16] T. Nakata, S. Komazaki, Y. Konho, H. Tanigawa, Effects of geometry and dimension of specimen and rig on small punch creep property, Exp. Mech. 57 (2017) 487-494.

[17] H. Kanayama, N. Hiyoshi, T. Itoh, F. Ogawa, T. Wakai, Effect of specimen size and oxygen partial pressure on creep characteristics of Mod. 9Cr-1Mo steel, J. Soc. Mater. Sci., 66 (2) (2017) 86-92.

[18] T. Itoh, Y. Irisawa, M. Sakane, Y. Kitamura. T. Tsurui, M. Fujiwara, T. Kim, Development of miniature creep testing for high temperature materials-Verification Testing, Proceedings of Third Conference on Small Sample Test Techniques-Determination of Mechanical Properties of Materials by Small Punch and Other Miniature Testing Techniques, Ostrava, Czech Republic, 2012, pp. 283.

[19] S. Zhang, Y. Takahashi, M. Sakane, Remaining life evaluation of long-term used Gr.91 using miniature creep specimen, 13th International Conference on Creep and Fracture of Engineering Materials and Structures, CREEP 2015, France, 2015.

[20] F.M. Huang, M.L. Hamilton, G.L. Wire, Bend testing for miniature discs, Nucl. Technol. 57 (1982) 234-242.

[21] M.P. Mahanan, A New Post-irradiation Mechanical Behavior Test: The Miniature Disk Bend Test, Nucl. Technol. 63 (1983) 275-295.

[22] X. Mao, H. Takahashi, Development of a further miniaturized specimen of 3 mm diameter for TEM disc (∅3 mm) small punch tests, J. Nucl. Materials. 150 (1987) 42-52.

[23] S. Komazaki, T. Tokunaga,Y. Kawaji, Small punch creep property of high Cr ferritic steels, Proceedings of the 3rd International conference of SSTT, Austria, 2014, 312-318.

[24] S. Komazaki, Y. Ohkawa, M. Yonemura, Effect of ductility on load/stress conversion coefficient of small punch creep test for Ni-base alloys, J-STAGE, DOI: 10.2355/tetsutohagane.TETSU-TETSU-2016-033.

[25] F.R. Larson, J. Miller, A time temperature relationship for rupture and creep stresses, Trans. ASME, 74 (1952) 765-775.

[26] J. Chakrabarty, A Theory of stretch forming over hemispherical punch heads, Int. J. Mech. Sci, 12 (1970) 315-325.

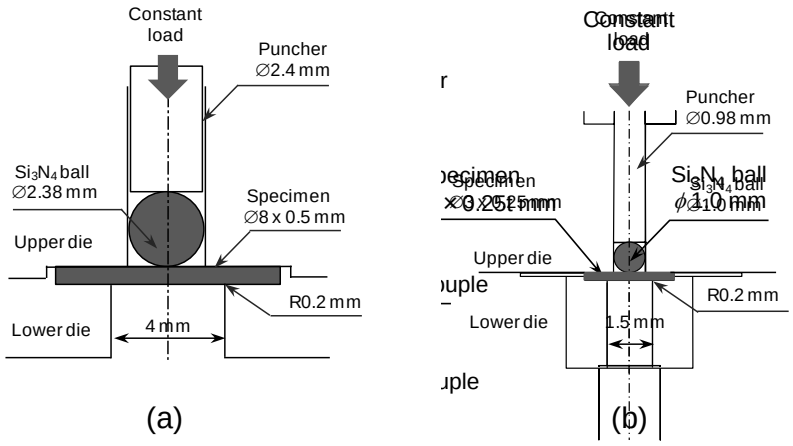

Figure 1. Schematic of SP creep test-rigs used for a) ∅8 mm and b) ∅3 mm specimens.

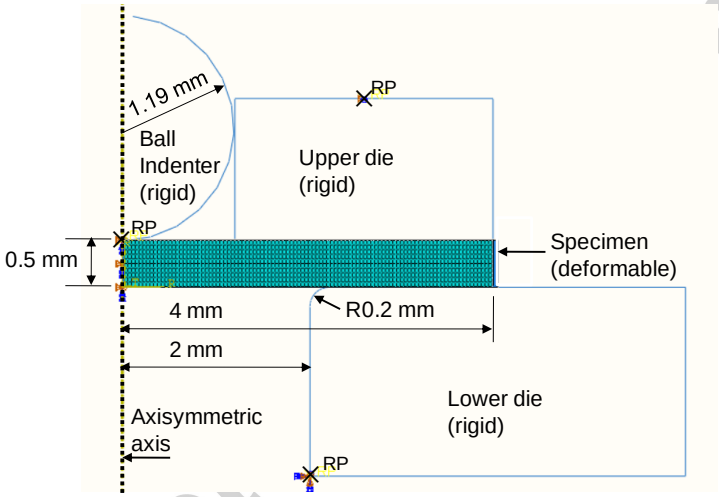

Figure 2. An example of axisymmetric FE model of SP creep test (∅8×0.5 mm specimen).

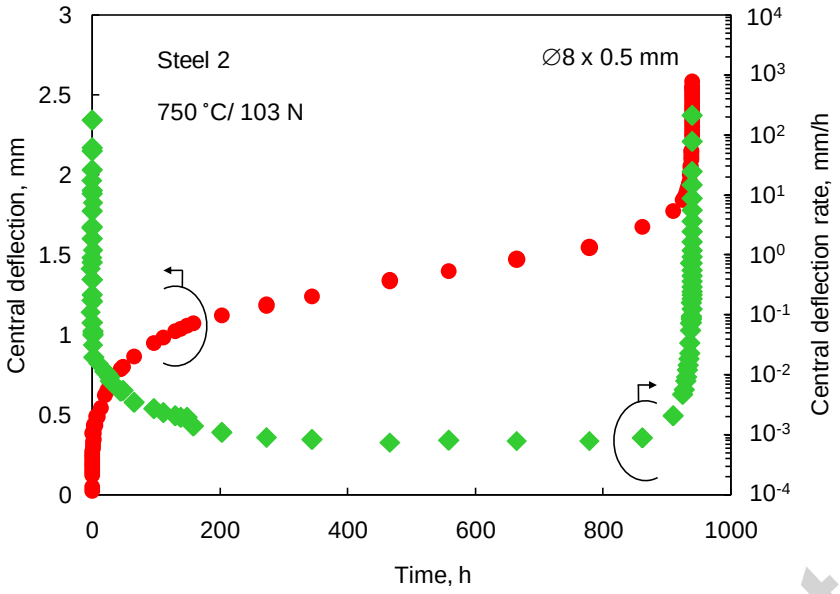

Figure 3. Representative central deflection-time and central deflection rate-time behavior for ∅8 mm specimen of steel 2.

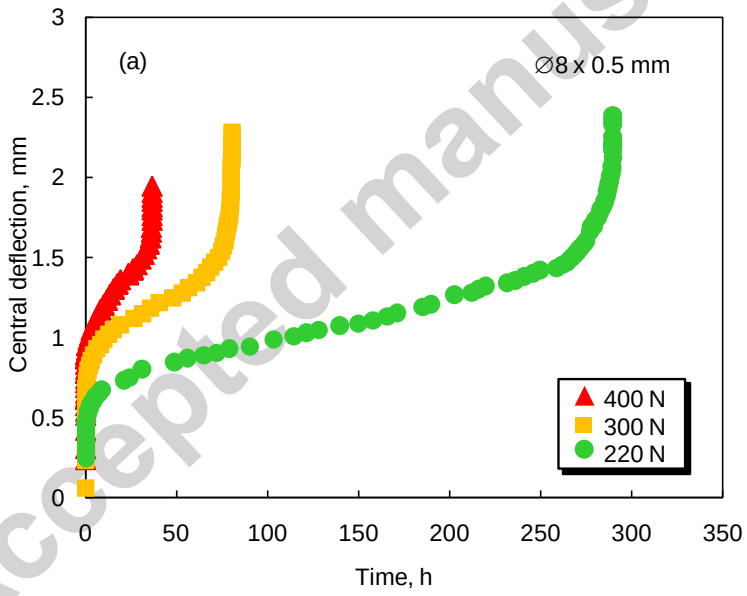

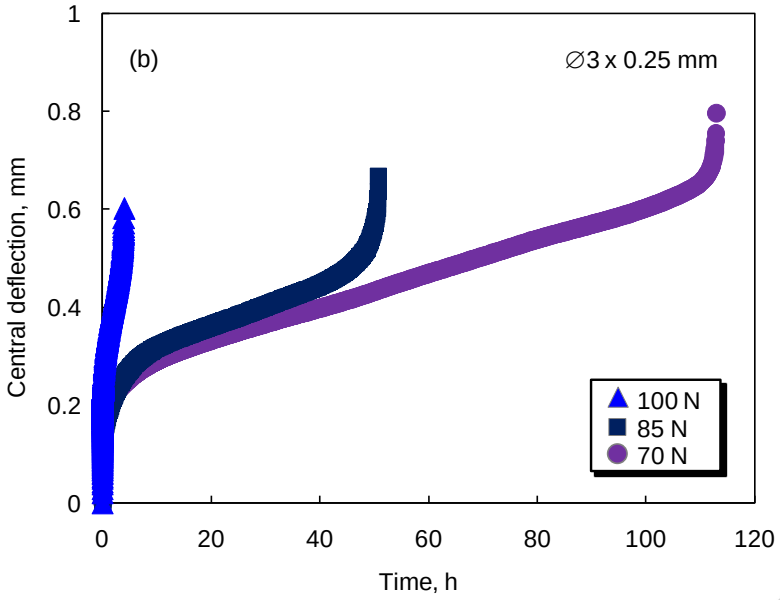

Figure 4. Central deflection-time behavior of a) ∅8 mm and b) ∅3 mm specimens at 700 ^{o}C under different loads, in steel 2.

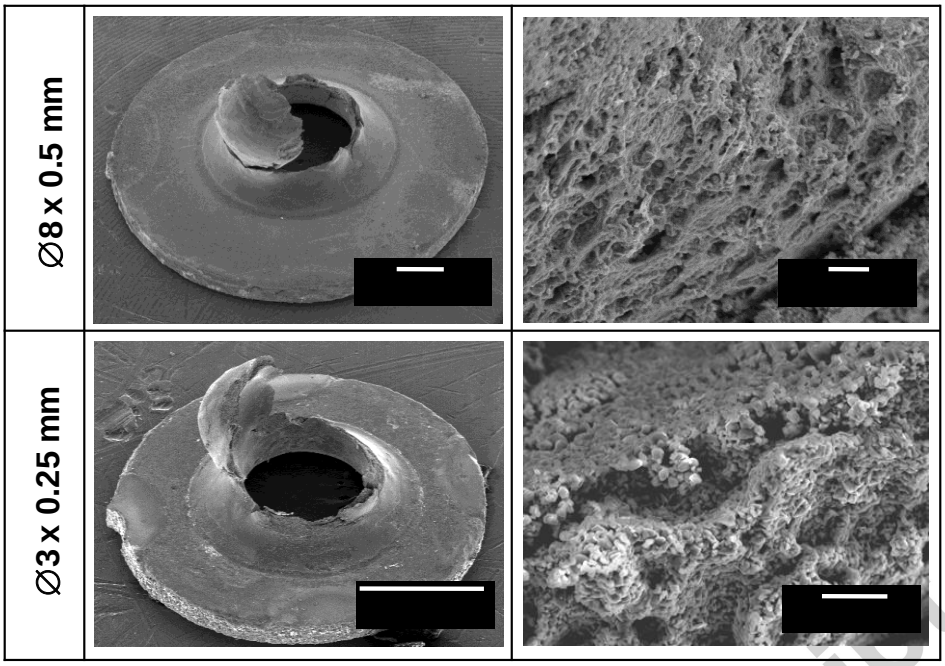

Figure 5. Fracture morphology of ∅8 mm and ∅3 mm SP specimens of steel 3 at 700 ˚C.

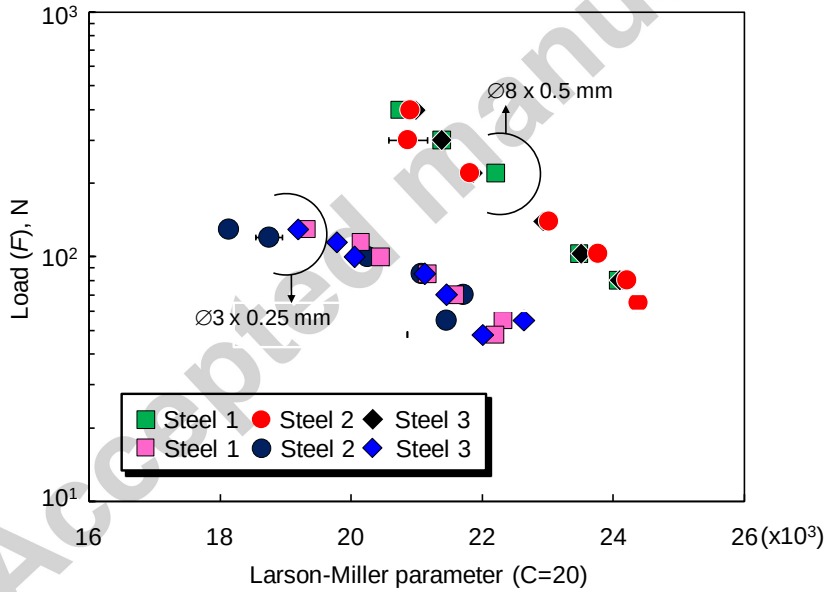

Figure 6. Comparison of creep rupture life of ∅8 mm and ∅3 mm specimens.

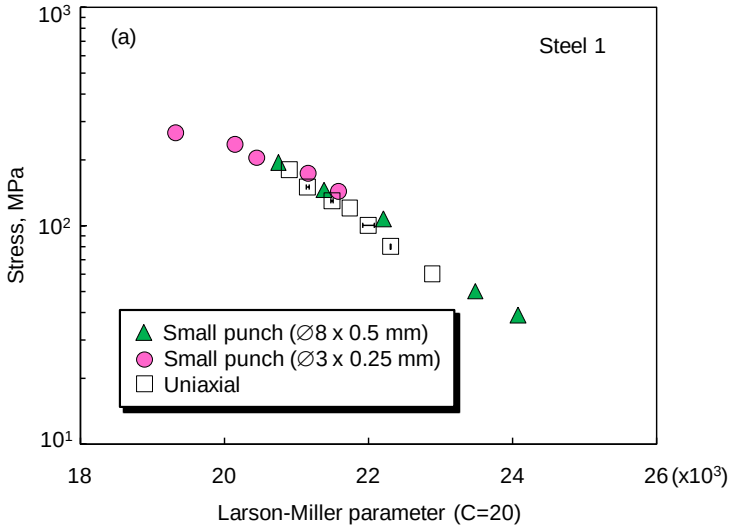

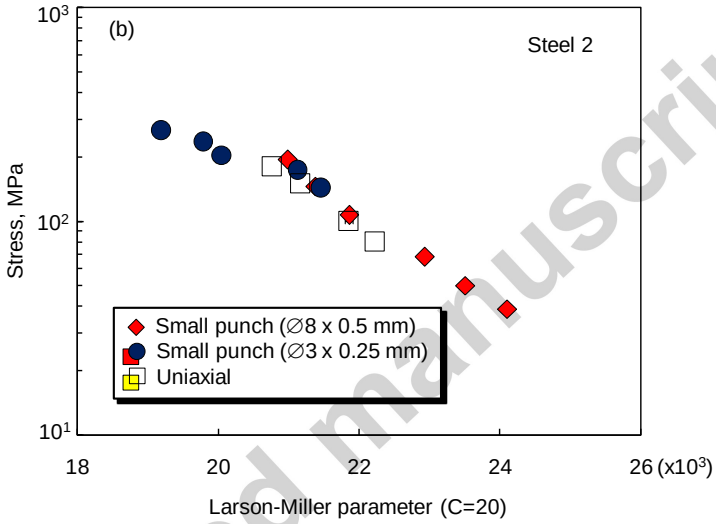

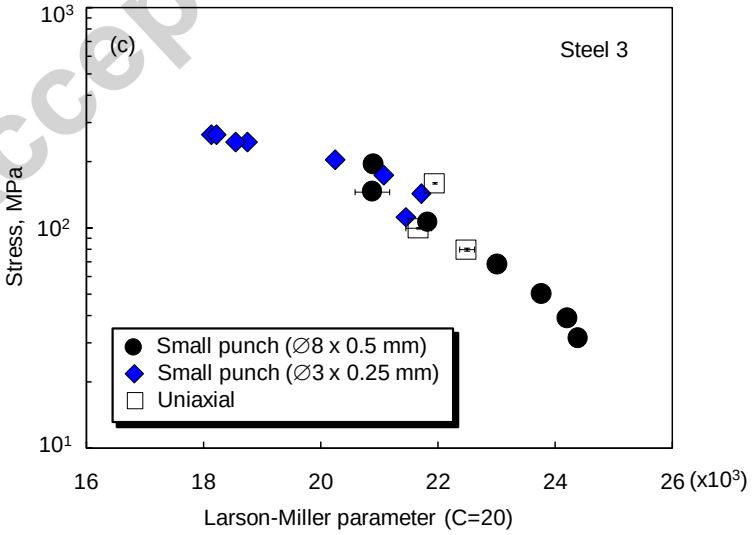

Figure 7. Correlation between SP and uniaxial creep rupture life for ∅8 mm and ∅3 mm specimens in a) steel 1, b) steel 2 and c) steel 3.

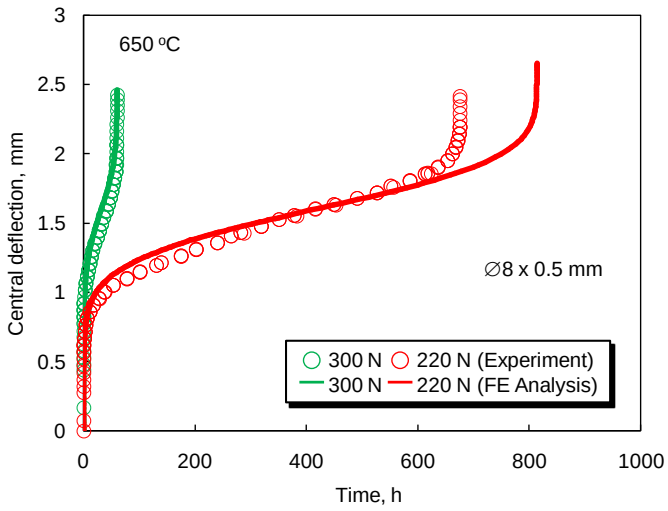

Figure 8. Typical central deflection-time behavior obtained from FE analysis in comparison with the experimental one at different loads.

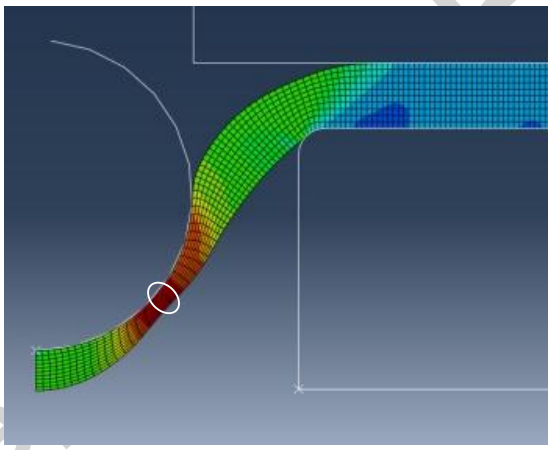

Figure 9. FE stress analysis result showing the region where maximum Von-Mises stress occurred on the outer surface of SP specimen.

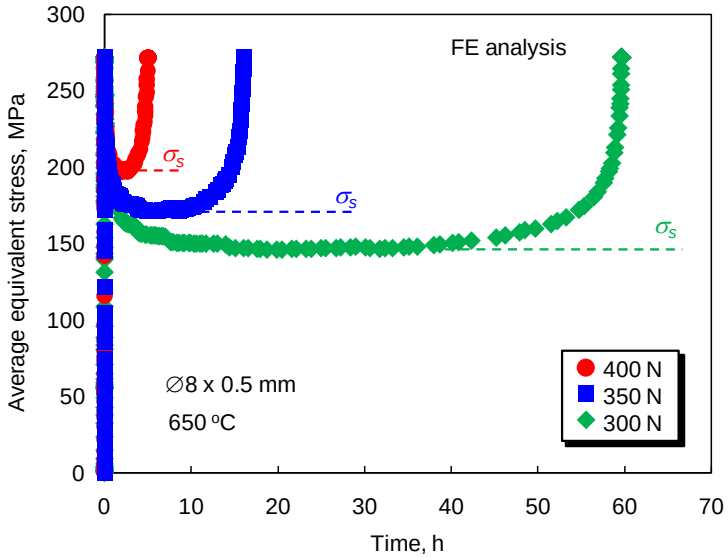

Figure 10. Typical variation of average equivalent stress with creep time at different loads.

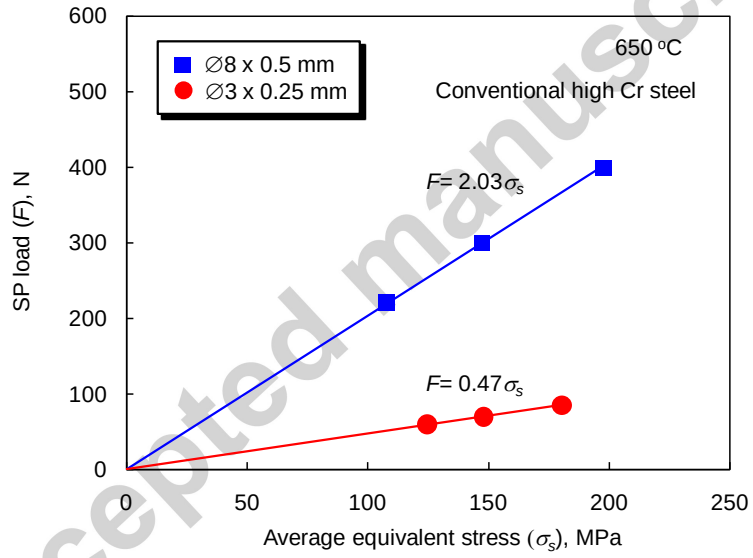

Figure 11. Relationship between the SP load (F) and average equivalent stress (σ_s) in ∅8 mm and ∅3 mm specimens in conventional high Cr steel.

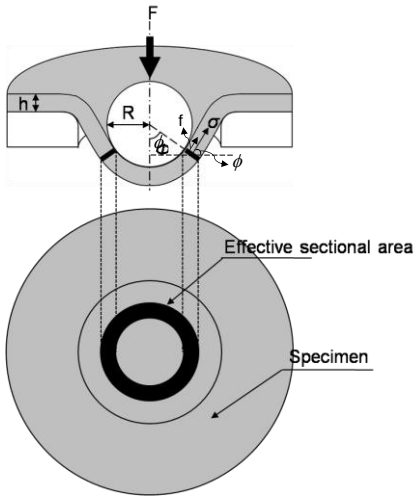

Figure. 12. Schematic illustration of SP creep deformation of the specimen.

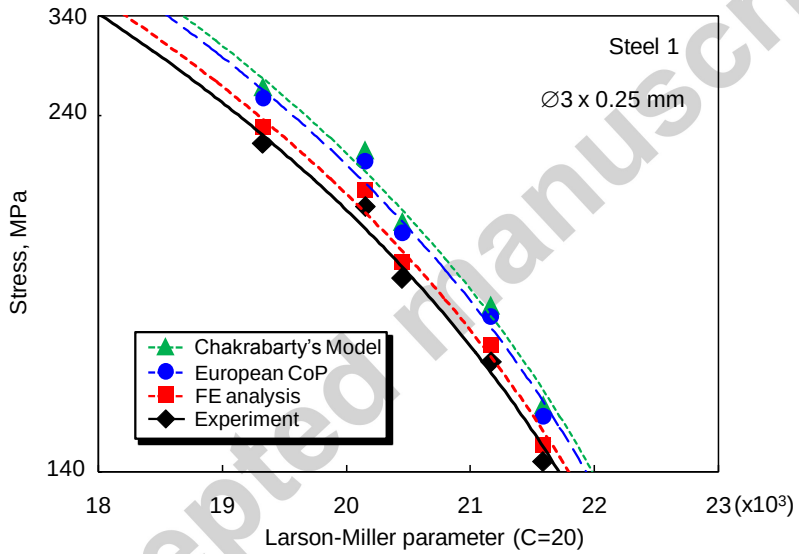

Figure 13. Comparison of predicted and experimental creep rupture life for ∅3 mm specimen in steel 1.

Table 1. Chemical compositions and heat treatment conditions of high nitrogen ferritic steels.

	Chemical composition (wt. %)											
Steels	C	N	Cr	Mo	V	Nb	W	Co	Mn	Ni	Si	Fe
Steel1/ Steel2	0.01	0.32	9.06	1.04	0.6	0.0[2]	5.97	4.0	0.07	0.01	0.06	balance
Steel3	0.015	0.34	15.0	1.0	1.3	0.02	6.0	4.0	0.07	0.01	0.06	balance

Steel1:1200 ^{o}C-30 min(air cooled) +780^{o}C-1 h (water quenched)
Steel2:1200^{o}C-30 min(air cooled) +700^{o}C-45 h (water quenched)
Steel3: 1200^{o}C-30 min (air cooled)

Table 2. Material properties used in FEA model.

E(GPa)	**$\sigma_{0.2}$ (MPa)**	**σ_B (MPa)**	**A (MPa^{-n}s^{-1})**	**n**	**ν**
109	177	272	2.9x10^{-24}	8.3	0.31

Table 3. Ratio of Load-stress conversion coefficients (Equations 6, 7, 8 and 9).

Chakrabarty	**CoP**	**FE analysis**	**Experiment**
4.67	4.57	4.32	4.18